GABARAPs regulate PI4P-dependent autophagosome:lysosome fusion

Hanzhi Wang[a,1], Hui-Qiao Sun[a,1], Xiaohui Zhu[a], Li Zhang[a], Joseph Albanesi[b], Beth Levine[c,d,e,2], and Helen Yin[a,2]

[a]Department of Physiology, [b]Department of Pharmacology, [c]Department of Internal Medicine, [d]Center for Autophagy Research, and [e]Howard Hughes Medical Institute, University of Texas Southwestern Medical Center, Dallas, TX 75390

Contributed by Beth Levine, April 17, 2015 (sent for review December 12, 2014; reviewed by Anne Simonsen)

The Atg8 autophagy proteins are essential for autophagosome biogenesis and maturation. The γ-aminobutyric acid receptor-associated protein (GABARAP) Atg8 family is much less understood than the LC3 Atg8 family, and the relationship between the GABARAPs' previously identified roles as modulators of transmembrane protein trafficking and autophagy is not known. Here we report that GABARAPs recruit palmitoylated PI4KIIα, a lipid kinase that generates phosphatidylinositol 4-phosphate (PI4P) and binds GABARAPs, from the perinuclear Golgi region to autophagosomes to generate PI4P in situ. Depletion of either GABARAP or PI4KIIα, or overexpression of a dominant-negative kinase-dead PI4KIIα mutant, decreases autophagy flux by blocking autophagsome:lysosome fusion, resulting in the accumulation of abnormally large autophagosomes. The autophagosome defects are rescued by overexpressing PI4KIIα or by restoring intracellular PI4P through "PI4P shuttling." Importantly, PI4KIIα's role in autophagy is distinct from that of PI4KIIIβ and is independent of subsequent phosphatidylinositol 4,5 biphosphate (PIP_2) generation. Thus, GABARAPs recruit PI4KIIα to autophagosomes, and PI4P generation on autophagosomes is critically important for fusion with lysosomes. Our results establish that PI4KIIα and PI4P are essential effectors of the GABARAP interactome's fusion machinery.

autophagy | GABARAP | PI4P | PI4KIIα | autophagosome:lysosome fusion

Macroautophagy (autophagy) is orchestrated by multiple autophagy-related (Atg) proteins (1). Among these, the Atg8 proteins are essential for autophagosome biogenesis and maturation. Mammals have at least six Atg8 orthologs that can be broadly classified into two large subfamilies: LC3s (light-chain 3) and GABARAPs (γ-aminobutyric acid receptor-associated proteins)/GATE-16s (Golgi-associated ATPase enhancer of 16 kDa), hereafter referred to collectively as GABARAPs. GABARAPs were initially identified as trafficking modulators for transmembrane receptors from the Golgi to the plasma membrane (2), and subsequently as Atg8s (1). Functional studies in mammalian cells have placed GABARAPs downstream of LC3 during autophagy (3).

The complexity of the mammalian Atg8 protein network was highlighted by a recent screen that revealed a cohort of at least 67 binding partners, a third of which are unique to either the LC3 or GABARAP families (4). Phosphatidylinositol 4-kinase IIα (PI4KIIα), which generates phosphatidylinositol 4-phosphate (PI4P) from phosphatidylinositol, was identified as a binding partner for GABARAPs, but not for LC3 (4). PI4KIIα is one of four vertebrate PI4Ks (5), and it has not been previously implicated in autophagy. Here we establish for the first time, to our knowledge, that GABARAPs govern the fusion of autophagosomes with lysosomes (A:L fusion) through PI4KIIα-mediated in situ PI4P generation on autophagosomes. We propose a working model that integrates GABARAPs' critical roles as trafficking modulators and autophagy effectors through PI4KIIα.

Results

Autophagy Induces PI4KIIα Translocation. Under normal growth conditions (Ctrl), PI4KIIα is concentrated in the perinuclear region and colocalizes with TGN46, a *trans* Golgi network (TGN) protein (Fig. 1*A*) (6). Short-term nutrient starvation in Earle's balanced salt solution (EBSS) promoted autophagy and induced PI4KIIα exit from the TGN. There was a decrease in PI4KIIα and TGN46 staining overlap and an increase in PI4KIIα puncta outside the Golgi. Anti-PI4P staining (7) showed that many of the scattered puncta also contained PI4P (Fig. 1*B*). The PI4P in the peripheral puncta is generated by PI4KIIα, because PI4KIIα depletion by small interfering (si) RNAs (6) decreased scattered PI4P puncta in EBSS-treated cells (Fig. 1*B* and Fig. S1).

Autophagosomes Contain PI4P and PI4KIIα. We used LC3 staining to identify autophagic structures (predominantly autophagosomes) and to determine whether they contain PI4P/PI4KIIα. As expected, in growing cells (Ctrl), LC3 was mostly cytosolic and present on the occasional autophagosomes formed by basal autophagy (Fig. 2*A*). Unlike PI4P, it was not concentrated in the perinuclear Golgi region. Starvation induced a large increase in the number of LC3 puncta that contained PI4P (Fig. 2*A*). Similar results were obtained by using the PI4P reporter, GFP-OSBP-PH [the PI4P binding pleckstrin homology (PH) domain of the oxysterol binding protein], to detect PI4P (Fig. 2*B*).

Many of the LC3 puncta also contained myc-PI4KIIα (Fig. 2*C*). The extent of colocalization, estimated by analysis of confocal Z stack images, was less than 10% in Ctrl growing cells and more than 60% in starved cells (Fig. 2*D*). Rapamycin (Rap), a mechanistic target of rapamycin (mTOR) inhibitor that induces autophagy, also generated autophagosomes containing PI4KIIα and the PI4P reporter (Fig. S2). In conclusion, PI4KIIα and PI4P are associated with many LC3-positive autophagic structures.

Significance

Autophagy is an essential homeostatic process that is critically important for maintaining health and that is dysregulated in multiple devastating diseases. The steps in the final stages of autophagy that culminate in autophagosome:lysosome fusion are not well understood. The γ-aminobutyric acid receptor-associated protein (GABARAP) family of Atg8 (autophagy-related 8) proteins has been implicated in autophagosome maturation. Here we report that phosphatidylinositol 4-kinase IIα (PI4KIIα), a lipid kinase that generates phosphatidylinositol 4-phosphate (PI4P) and binds GABARAPs, is recruited to autophagosomes by GABARAPs. Furthermore, PI4P generation by PI4KIIα, but not by PI4KIIIβ, another major mammalian PI4K, promotes autophagosome fusion with lysosomes. Our results establish for the first time to our knowledge that PI4KIIα is a specific downstream effector of GABARAP and that PI4P has a key role in the final stage of autophagy.

Author contributions: H.W., H.-Q.S., X.Z., L.Z., J.A., B.L., and H.Y. designed research; H.W., H.-Q.S., X.Z., and L.Z. performed research; H.W., H.-Q.S., X.Z., L.Z., J.A., B.L., and H.Y. analyzed data; and H.Y. wrote the paper.

Reviewers included: A.S., University of Oslo.

The authors declare no conflict of interest.

Freely available online through the PNAS open access option.

[1]H.W. and H.-Q.S. contributed equally to this work.

[2]To whom correspondence may be addressed. Email: Beth.Levine@utsouthwestern.edu or Helen.Yin@UTSouthwestern.edu.

This article contains supporting information online at www.pnas.org/lookup/suppl/doi:10.1073/pnas.1507263112/-/DCSupplemental.

CELL BIOLOGY

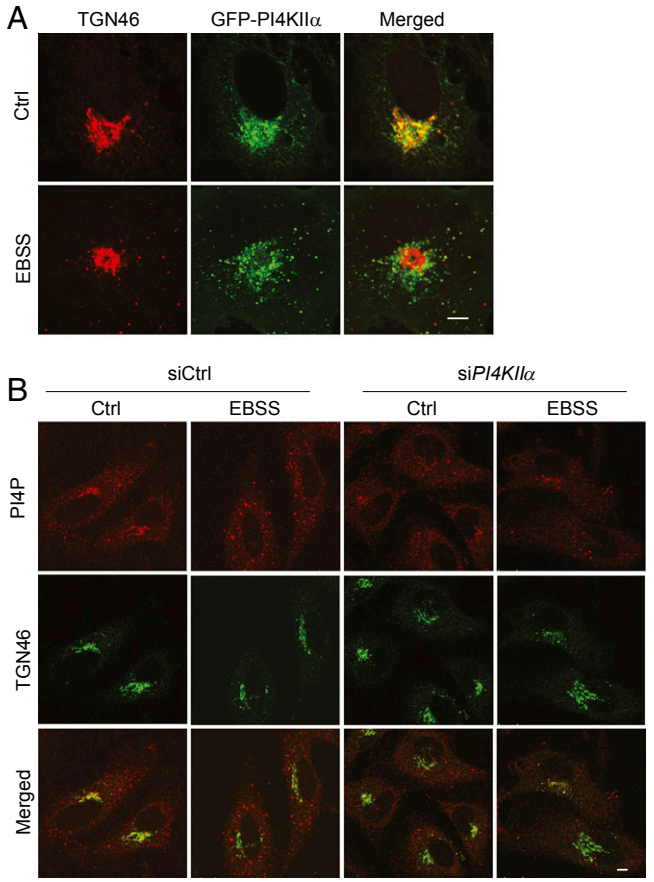

Fig. 1. Autophagy induces PI4KIIα redistribution to cytoplasmic puncta. (Scale bar, 5 μm.) (*A*) PI4KIIα and TGN46 localization. COS cells stably expressing GFP-PI4KIIα were exposed to growth medium (Ctrl) or EBSS and stained with anti-TGN46 (red). (*B*) si*PI4KIIα* decreased peripheral PI4P puncta in starved HeLa cells.

PI4KIIα Translocation to Autophagosomes Is Palmitoylation-Dependent. PI4KIIα is palmitoylated on a cysteine-rich motif (^{174}CCPCC^{178}) in the Golgi and behaves like an integral membrane protein that is associated with cholesterol-rich lipid raft microdomains (8, 9). The nonpalmitoylable myc-PI4KIIα mutant in which all of the cysteines in the CCPCC motif were replaced by serines (SSPSS) is predominantly cytosolic and nonraft-associated and ectopically associates with membranes as a peripheral protein (8, 9). Significantly, it was not enriched in autophagosomes (Fig. 2*E* and Fig. S2*B*), detected either by staining endogenous LC3 in HeLa cells (Fig. 2*E*) or GFP-LC3 in HeLa cells stably expressing GFP-LC3 (HeLa/GFP-LC3) (Fig. S2*B*). These results establish that PI4KIIα recruitment to autophagosomes is palmitoylation-dependent.

PI4KIIα Depletion Generates Abnormally Large Autophagosomes. When HeLa/GFP-LC3 cells were maintained in Opti-Eagle's minimal essential medium (MEM)/5% (vol/vol) FBS to minimize basal autophagy, GFP-LC3 was diffusely cytosolic and nuclear (Fig. 3*A*). EBSS or Rap induced formation of small GFP-LC3 puncta in siCtrl cells and much larger puncta in si*PI4KIIα* cells. Quantitative image analysis showed that the si*PI4KIIα* cells had five- and three-fold higher residual GFP-LC3 at the end of treatment, respectively (Fig. 3*A*). Because the HeLa/GFP-LC3 cells expressed similar amounts of GFP-LC3 initially before autophagy induction, we conclude that si*PI4KIIα* blocks GFP-LC3 degradation to increase puncta size. Likewise, si*PI4KIIα* also generated large autophagosomes in cells expressing only endogenous LC3 (Fig. 3*A*, *Middle*).

The GFP-LC3 puncta have a unimodal area distribution in autophagic siCtrl cells and a bimodal distribution in si*PI4KIIα* cells (Fig. 3*A*). The coexistence of normal-sized and enlarged autophagosomes in si*PI4KIIα* cells raises the possibility that autophagosomes may have formed normally initially, but are defective at a later stage, culminating in enlargement. Transmission electron microscopy showed that the enlarged structures were double-membrane vesicles that contained organelles and assorted cytoplasmic materials (Fig. 3*B*, *Top*). Thus, they are bona fide autophagosomes and not single-membrane amphisomes generated by endosome fusion with autophagosomes (10). Correlative light and electron microscopy confirmed that the enlarged structures contained GFP-LC3 (Fig. 3*B*, *Bottom*). Interestingly, similar to PI4KIIα depletion, GABARAP depletion also generated enlarged autophagosomes, suggesting they may be functionally related. This possibility is confirmed in experiments described here.

PI4KIIα Depletion or Kinase-Dead PI4KIIα Overexpression Inhibits Autophagy Flux. We used Western blotting to determine that si*PI4KIIα* cells had decreased LC3 autophagy flux (3) that could explain their enlarged autophagosome phenotype. Control growing cells had predominantly LC3-I (cytosolic) and a small amount of lipidated LC3-II (Fig. 3*C*). EBSS increased LC3-I conversion to LC3-II, which is degraded after A:L fusion. Bafilomycin A1 (Baf A1) increased LC3-II steady state levels in siCtrl cells by blocking its degradation in autolysosomes. In contrast, starved si*PI4KIIα* cells had more LC3-II than Ctrl cells, and Baf A1 did not increase LC3-II levels much further. Quantitative Western blotting showed that the starved si*PI4KIIα* cells had an ∼150% increase in final LC3 levels and a more than 90% decrease in the extent of LC3 degradation

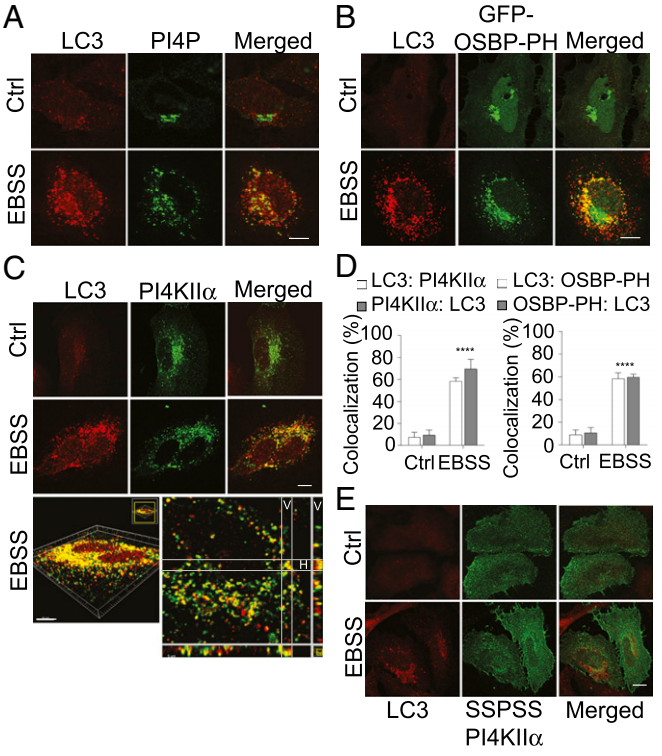

Fig. 2. LC3 autophagosomes contain PI4P and PI4KIIα. HeLa cells were exposed to growth medium (Ctrl) or EBSS. (Scale bars, 10 μm.) (*A*) LC3 (red) and anti-PI4P (green). (*B*) LC3 (red) and GFP-OSBP-PH (a PI4P reporter). (*C*) LC3 (red) and myc-PI4KIIα (green). (*Top*) Images from a single confocal plane. (*Bottom*) Serial stack of an EBSS-treated cell. The red and green components in multiple planes were analyzed in the vertical (V) and horizontal (H) dimensions. (*D*) Imaris AutoQuant (Bitplane) colocalization analysis. Z stacks from 20 cells similar to those shown in *C* were analyzed for each data point. Percentages LC3 colocalization with myc-PI4KIIα or GFP-OSBP-PH and vice versa are shown (mean ± SEM; ****$P < 0.001$). (*E*) LC3 and the nonpalmitoylable SSPSS myc-PI4KIIα.

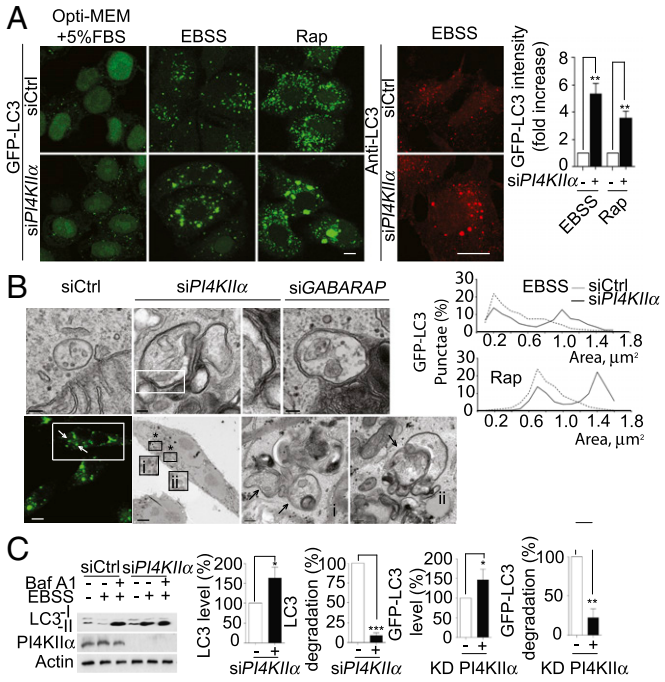

Fig. 3. Effects of PI4KIIα depletion or KD PI4KIIα overexpression on autophagosome size and autophagy flux. (*A*) PI4KIIα-depletion. (*Left*) GFP-LC3 in HeLa/GFP-LC3 cells exposed to different conditions. (*Right*) Endogenous LC3 in starved HeLa cells. Bar graph, quantitation of GFP-LC3 fluorescence in HeLa/GFP-LC3 cells after EBSS or Rap treatment. The *y* axis shows GFP-LC3 intensities remaining in si*PI4KIIα* relative to siCtrl (set at a value of 1) cells (mean ± SEM; $n = 3$; $^{**}P < 0.001$). Fifty cells per condition. Area distribution, GFP-LC3 puncta areas (μm^2) from 20 cells per condition were determined by ImageJ area analysis (mean ± SEM; $n = 3$). (*B*) Representative electron micrographs. EBSS-treated HeLa/GFP-LC3 cells were processed for transmission electron microscopy (*Top*) or for correlative light and electron microscopy (*Bottom*). (Scale bars, 100 nm.) The area enclosed by the rectangle in the top row is enlarged in the third panel to show the vesicle's double limiting membranes. (*Bottom*, *Left* to *Right*): first panel, GFP-LC3 fluorescence in starved si*PI4KIIα* HeLa/GFP-LC3 cells. (Scale bar, 10 μm.) Rectangle highlights a representative cell selected for correlative electron microscopy. Second panel, a low-magnification electron micrograph. (Scale bar, 5 μm.) The regions highlighted by an asterisk (i and ii) are enlarged in the last two panels. Arrows, autophagosomes. (Scale bars, 200 nm.) (*C*) Autophagy flux. (*Left*) Western blot of endogenous LC3, PI4KIIα, and actin without and with EBSS. Cells were incubated with Baf A1 (100 nM, 12 h) and exposed to EBSS for the last 2 h. (*Right*) Quantitation of Western blot. LC3 remaining and percentage LC3 degradation were normalized against actin content and expressed relative to siCtrl cells set as 100%. Values are percentage mean ± SEM ($n = 3$). $^{*}P < 0.05$; $^{**}P < 0.01$; $^{***}P < 0.001$.

(Fig. 3*C*). Degradation of p62/sequestome 1 (SQSTM1), another autophagy substrate, was also impaired (Fig. S3*A*).

The kinase dead (KD) myc-PI4KIIα Lys115Met (K151M) substitution mutant, which is raft-associated and correctly targeted to endomembranes in growing cells (8, 9), was also recruited to autophagosomes (Fig. S3*A*). Furthermore, high-level KD PI4KIIα overexpression generated enlarged autophagosomes and decreased degradation of GFP-LC3 and autophagy flux (Fig. 3*C* and Fig. S3*B*). Therefore, it acted as a dominant negative inhibitor to replicate the PI4KIIα depletion phenotype. We conclude that PI4KIIα generation of PI4P on autophagosomes is required in addition to any potential scaffolding functions.

PI4KIIα Depletion Inhibits Acidification and A:L Fusion. To determine whether the block in autophagic flux is a result of decreased autophagosome fusion with lysosomes (A:L fusion) at late-stage autophagy (10), we used several approaches. First, the tandem monomeric red fluorescent protein (mRFP)-GFP-LC3, which capitalizes on the higher sensitivity of GFP to quenching by acidic pH than mRFP (11), was used to determine whether there is a decreased rate of autophagosome acidification. siCtrl cells showed a time-dependent decrease in unfused (yellow) autophagosomes in EBSS, whereas si*PI4KIIα* cells had much slower rates of decrease (Fig. 4*A*). Similar results were obtained with Rap. Because there was no obvious change in LysoTracker staining (Fig. S4*A*), this decrease is not likely to be a result of gross lysosomal/endosomal acidification defects per se.

Second, live cell imaging was used to examine the dynamics of A:L fusion. Previous studies have shown that autophagosomes engage in homotypic and heterotypic fusions, including complete fusion with lysosomes to form autolysosomes, kiss-and-run fusion, and extension of tubules to reach targets (12). Under our experimental conditions, complete heterotypic fusions predominated. For example, in the time-lapse frames for Ctrl cells (Fig. 4*B*, sequence 1), the green LC3 and red lysosomal-associated membrane protein 1 (LAMP1) puncta formed a hybrid yellow autolysosome by the 130-s frame. Subsequently, the yellow puncta turned red, most likely as a result of quenching of GFP-LC3 fluorescence in the acidic autolysosomes (also see Fig. S4*B* and Movie S1). In contrast, in si*PI4KIIα* cells, the majority of autophagosomes did not fuse with lysosomes (Fig. 4*B*, sequence 2). In some cases, autophagosomes transiently contacted lysosomes (e.g., at 410 s) but rapidly separated (Fig. S4*B* and Movies S2 and S3). Particle tracking analyses showed that the contact periods between the pairs in PI4KIIα-depleted cells ranged from 5 to 35 s (mean ± SEM: 16 ± 6 s; $n = 5$). Interestingly, some vesicle pairs with long apparent dwell times underwent successive rounds of partial "engagement and disengagement" before completely separating (Fig. S4*B* and Movie S4). Occasionally, some large LC3 autophagosomes extended tubules to contact lysosomes but did not fuse (Fig. 4*B*, sequence 3, Fig. S4*B*, and Movie S3). Taken together, our results established that PI4KIIα depletion inhibits autophagosome acidification by blocking A:L fusion.

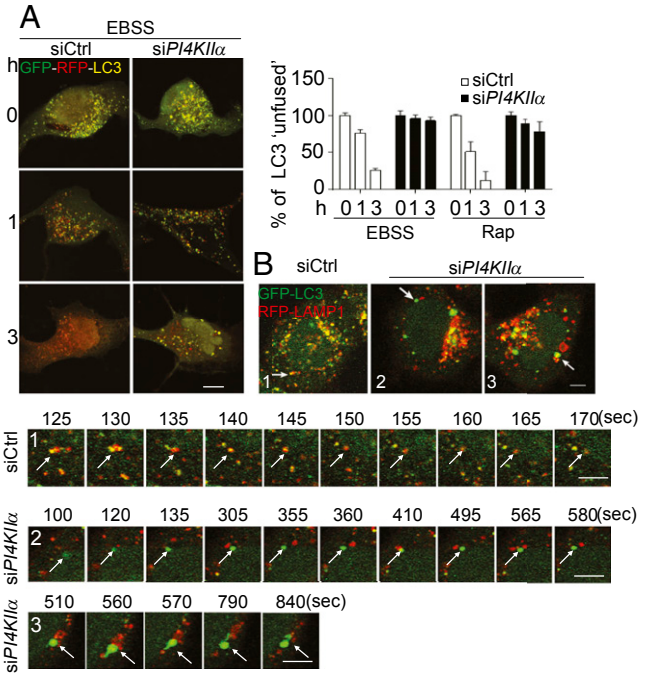

Fig. 4. PI4KIIα depletion inhibits A:L fusion. (Scale bars, 5 μm.) (*A*) Acidification. HeLa cells expressing mRFP-GFP-LC3 were treated with Baf A1 for 12 h. After Baf A1 washout, cells were exposed to EBSS or Rap. Images were collected from cells fixed at 0, 1, or 3 h (Rap images in Fig. S4*A*). Bar graphs, percentage yellow (unfused) LC3 puncta relative to total red puncta (mean ± SEM; 60 cells per assay, $n = 3$). (*B*) Time-lapse microscopy. siCtrl or si*PI4KIIα* HeLa/GFP-LC3 cells were retransfected with pDSRED-LAMP1, starved, and subjected to time-lapse microscopy. Arrows indicate A:L pairs in the time-lapse frames.

GABARAPs Recruit PI4KIIα to Autophagosomes. Because PI4KIIα coimmunoprecipitated with GABARAPs (4), we determined they are functionally related in autophagy. Coimmunoprecipitation assays confirmed that PI4KIIα bound GFP-GABARAPs, but not GFP-LC3 (Fig. 5*A* and Fig. S5*A*). Furthermore, they were colocalized in autophagic cells (Fig. 5*A*). The shortest N- and C-terminal truncated myc-PI4KIIα tested (aa 92–397) that bound GFP-GABARAP contains both the catalytic and palmitoylation motif (8) (Fig. 5*A*). Unexpectedly, SSPSS myc-PI4KIIα, which is neither palmitoylated nor autophagosome-associated (Fig. 2*E*), also coimmunoprecipitated with GFP-GABARAP. Thus, PI4KIIα interaction with GABARAPs is necessary but not sufficient for autophagosome targeting. Additional studies will be required to determine what is required for PI4KIIα targeting, and what for preferential binding to GABARAPs.

We compared the effect of depleting either player on each other's behavior to delineate their upstream/downstream relations. si*PI4KIIα* generated large GFP-LC3 puncta that contained YFP-GABARAP and mCherry-GATE-16 (Fig. 5*B* and Fig. S5*B*) to a similar extent as in siCtrl cells (Fig. 5*C*). In contrast, although si*GABARAP*s depletion (3) (Fig. S5*C*) also generated enlarged autophagosomes, these abnormal autophagosomes were deficient in both PI4KIIα and PI4P (Fig. 5 *C* and *D* and Fig. S5*B*). Because the large autophagosomes in si*GABARAP* cells have similar ultrastructural features as in si*PI4KIIα* cells (Fig. 3*B*), GABARAPs are placed upstream of PI4KIIα. Thus, GABARAPs are recruited to autophagosomes independent of PI4KIIα, and they recruit PI4KIIα to autophagosomes in a palmitoylation-dependent manner.

PI4KIIα Acts Downstream of GABARAPs. To confirm this hierarchy, we examined whether overexpression of the putative downstream effector (PI4KIIα) compensates for the depletion of the upstream

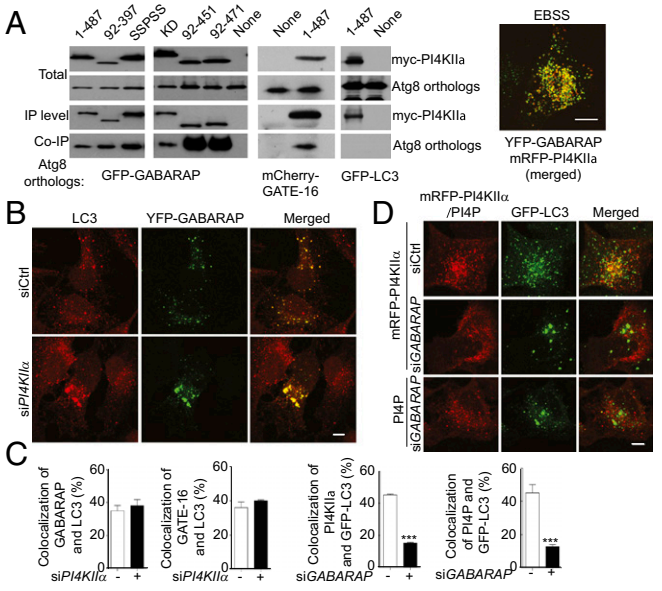

Fig. 5. Hierarchical relation between PI4KIIα and GABARAPs. (*A*) Coimmunoprecipitation and colocalization. (*Left*) HEK-293 cells overexpressing myc-PI4KIIα variants together with GFP-GABARAP or mCherry-GATE-16 were subjected to immunoprecipitation with anti-myc, and coimmunoprecipitated tagged proteins were detected with anti-GFP or anti-mCherry. (*Right*) Representative merged image of YFP-GABARAP and mRFP-PI4KIIα in a starved cell. (Scale bar, 10 μm.) (*B*) si*PI4KIIα* effects on GABARAP:LC3 colocalization in starved PI4KIIα-depleted HeLa cells that expressed low levels of YFP-GABARAP. (Scale bars, 10 μm.) (*C*) Colocalization. Sixty cells were analyzed per data point. Values are mean ± SEM ($n = 3$); ***$P < 0.001$. (*D*) si*GABARAP* effects on mRFP-PI4KIIα and PI4P colocalization with GFP-LC3. Top two rows: mRFP-PI4KIIα (red) and GFP-LC3; bottom row: anti-PI4P (red) and GFP-LC3. (Scale bar, 5 μm.)

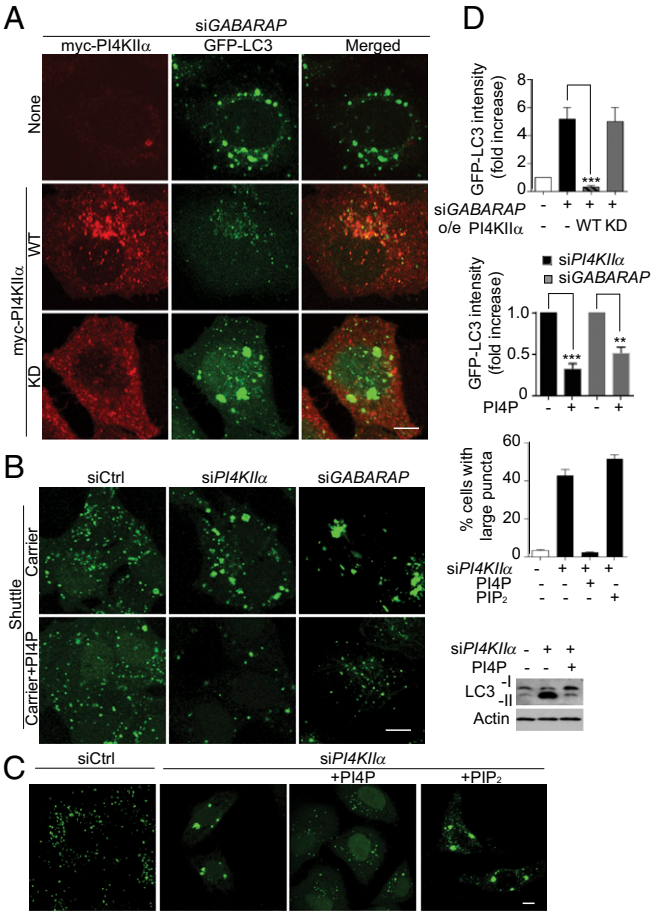

Fig. 6. PI4KIIα and PI4P act downstream of GABARAPs. HeLa/GFP-LC3 cells (except as noted) transfected with si*GABARAP* or si*PI4KIIα* and manipulated further were starved in EBSS. (Scale bars, 5 μm.) (*A*) Overexpression of WT but not KD myc-PI4KIIα rescued the large autophagosome phenotype in si*GABARAP* cells. HeLa/GFP-LC3 cells were stained with anti-myc (red). (*B*) Rescue by PI4P shuttling. Images show GFP-LC3 puncta in cells with shuttle carrier ± PI4P for 2 h in EBSS. Western blot shows endogenous LC3 in EBSS-starved HeLa cells. (*C*) Differential effects of PI4P or PIP_2 shuttling. (*D*) Quantitation. Top two bar graphs: GFP-LC3 puncta fluorescence intensity. Values are mean ± SEM ($n = 3$; 60 cells per condition; **$P < 0.01$; ***$P < 0.001$), with control set at 1. Bottom bar graph: percentage of cells with large LC3 puncta. Values are mean ± SEM ($n = 4$, 40 cells per condition).

controllers (GABARAPs). Overexpression of WT myc-PI4KIIα decreased accumulation of enlarged autophagosomes and GFP-LC3 puncta intensity in si*GABARAP* cells (Fig. 6 *A* and *D*). Rescue is dependent on PI4P generation, because KD myc-PI4KIIα did not rescue. We hypothesize that PI4KIIα overexpression may have rescued the si*GABARAP* phenotype by increasing promiscuous, GABARAP-independent PI4KIIα association/PI4P generation in all membranes.

PI4P "shuttling" (6) was used to determine whether the si*PI4KIIα* or si*GABARAP*s autophagy block is a direct result of PI4P depletion. PI4P shuttling decreased the size of the GFP-LC3 puncta and also promoted GFP-LC3 degradation, as assessed by GFP-LC3 staining intensity (Fig. 6*C*) and by LC3 Western blotting (Fig. 6*D*). In contrast, PIP_2 shuttling did not rescue. These results establish conclusively that PI4P directly promotes A:L fusion directly and independent of its subsequent conversion to PIP_2.

PI4KIIα and PI4KIIIβ Have Different Roles in Autophagy. Because we showed that PI4KIIα promotes A:L fusion and is present on autophagosomes, we next asked whether PI4KIIα is also constitutively associated with lysosomes. We found that in growing cells,

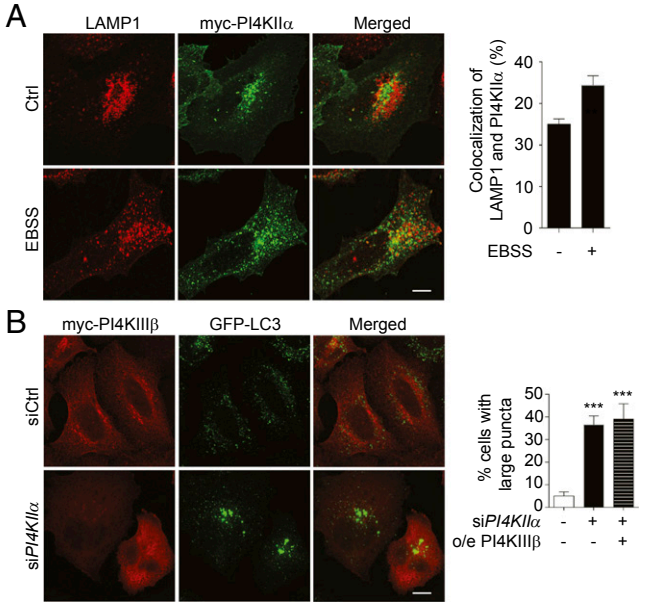

Fig. 7. PI4KIIα has a unique role in autophagy. (*A*) Effect of starvation on colocalization of PI4KIIα with LAMP1. HeLa cells transiently overexpressing myc-PI4KIIα with and without starvation were stained with anti-myc and anti-LAMP1. (Scale bars, 10 μm.) Bar graph, colocalization was determined using the Zeiss LSM510 software ($n = 3$, $^{**}P < 0.02$). (*B*) Myc-PI4KIIIβ overexpression fails to rescue the si*PI4KIIα* phenotype. HeLa/GFP-LC3 cells sequentially transfected with *PI4KIIα* or Ctrl siRNA and myc-PI4KIIIβ were exposed to EBSS. Bar graph, percentage si*PI4KIIα* cells with large LC3 puncta. Sixty cells were analyzed per condition ($n = 4$; $^{***}P < 0.001$).

only ∼25% of PI4KIIα colocalized with LAMP1, a lysosome and late endosome marker, and colocalization increased to ∼35% in starved cells (Fig. 7 *A* and *B*). Because the extent of colocalization is much less than that for PI4KIIα/LC3 (Fig. 2*B*), PI4KIIα most likely resides primarily on autophagosomes and is transferred to autolysosomes after A:L fusion.

Because PIP5Kβ, which generates PIP_2 from PI4P, and PI4KIIIβ, the only PI4K that has been previously implicated in autophagy, promote autophagic lysosome reformation downstream of A:L fusion (13, 14), we compared the effect of their depletion (documented in Fig. S6*A*) with that of PI4KIIα depletion. As expected, the large GFP-LC3 autophagosomes in PI4KIIα-depleted cells had decreased overlap with LAMP1 (Fig. S6*B*). In contrast, neither si*PIP5Kβ* nor si*PI4KIIIβ* affected LAMP1:GFP-LC3 colocalization to a similar extent. Significantly, myc-PI4KIIIβ neither translocated to autophagosomes nor rescued the enlarged autophagosomes in si*PI4KIIα* cells (Fig. 7*B*). Thus, PI4KIIα is uniquely poised to control A:L fusion using a mechanism distinct from that of PI4KIIIβ, and without a requirement for downstream PIP_2 generation.

Discussion

We establish that GABARAPs recruit palmitoylated PI4KIIα from the Golgi to autophagosomes, and that PI4P generation in situ promotes A:L fusion. Our results raise the intriguing and hitherto unexplored possibility that GABARAPs' role in autophagosome maturation may be integrated with their established role as modulators of transmembrane protein trafficking. The requirement for GABARAPs, PI4KIIα, and PI4P for A:L fusion was established using multiple approaches. Because autophagosomes undergo homotypic as well as heterotypic fusions (12), we hypothesize that the abnormally large autophagosomes in si*GABARAP* and si*PI4KIIα* cells may have been generated by multiple default homotypic fusion events when heterotypic fusion is blocked.

GABARAPs are placed upstream of PI4KIIα and PI4P, and our working model is summarized in Fig. 8. GABARAP depletion generates enlarged autophagosomes that are PI4KIIα- and PI4P-deficient and have decreased autophagic flux. The GABARAP depletion phenotype can be rescued either by overexpressing WT PI4KIIα (but not KD PI4KIIα) or by shuttling PI4P. Thus, PI4P generation, and not simply tethering by PI4KIIα within the GABARAP interactome, is required. Because rescue occurs even in the absence of GABARAPs, GABARAPs' primary role in this context is to increase PI4P. PI4KIIα depletion also generated enlarged autophagosomes that contain GABARAPs, but not PI4P, placing it downstream of GABARAPs. This phenotype can be rescued by PIP, but not PIP_2, shuttling. Unlike PI4KIIα, PI4KIIIβ does not reside on autophagosomes and fails to rescue the enlarged autophagosome phenotype in PI4KIIα-depleted cells. Thus, PI4KIIα is uniquely responsible for promoting A:L fusion.

We further propose that GABARAPs recruit PI4KIIα to autophagosomes through vesicular trafficking from the Golgi because, first, PI4KIIα is palmitoylated primarily at the Golgi (8, 9), and only palmitoylated PI4KIIα translocates to autophagosomes. GABARAPs may direct trafficking of palmitoylated PI4KIIα from the Golgi to autophagosomes, analogous to their previously identified role as facilitators of $GABA_A$ trafficking to the plasma membrane (2). Second, PI4KIIα has already been implicated in constitutive exocytic, endo/lysosomal trafficking (6, 15, 16), and its recruitment to autophagosomes is decreased by GABARAP depletion. Third, there is emerging evidence that lipids enriched in raft microdomains may be involved in autophagosome maturation. Finally, trafficking of Golgi and late/recycling endosomes, which are rich in

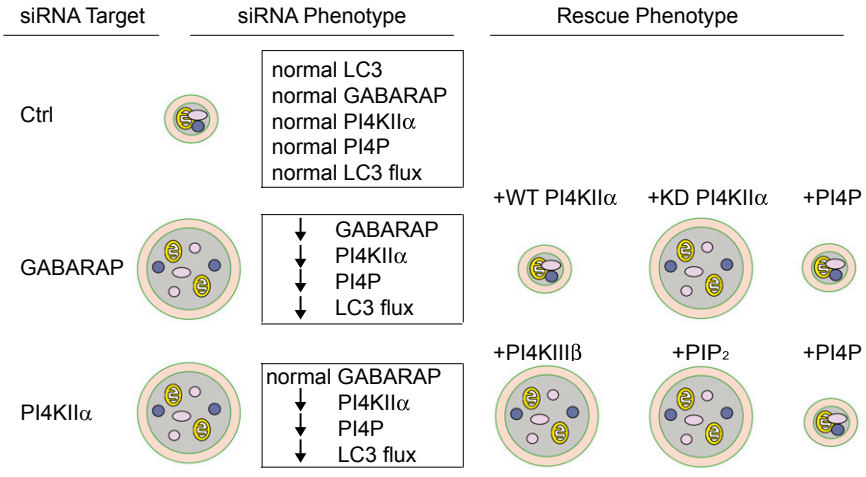

Fig. 8. Summary of results and proposed hierarchy in the GABARAP interactome. PI4KIIα or GABARAP depletion individually blocks A:L fusion, resulting in accumulation of enlarged autophagosomes. GABARAPs and PI4KIIα cooperate to ensure in situ generation of PI4P on autophagosomes to promote A:L fusion. The hierarchical relationships among GABARAPs, PI4KIIα, and PI4P are delineated by depletion and rescue approaches. Circles with double membranes are autophagosomes containing random cytoplasmic material and organelles.

CELL BIOLOGY

raft-associated PI4KIIα, contributes to intermixing of membranes, leading to autophagosome expansion (1).

Our results raise the fundamental question of how the GABARAP/PI4KIIα/PI4P interactome regulates the A:L fusion machinery. Previous studies have shown that particle docking and fusion are independent steps (12) and that the GABARAP scaffolding network promotes cargo recruitment, tethering, and potentially membrane fusion (3). Our live cell imaging studies reveal that autophagosomes and lysosomes in PI4KIIα-depleted cells occasionally exhibit a transient and repetitive partial engagement/disengagement behavior that is different from straightforward kiss-and-run. This unusual behavior suggests that stable docking and membrane hemifusion may be compromised.

Because shuttled PI4P rescued the effects of depleting either GABARAPs or PI4KIIα in late-stage autophagy, PI4P is strongly implicated in promoting late-stage autophagy. By analogy to PI3P, which regulates early-stage autophagy by creating a platform to recruit specific effectors, PI4P may provide a platform for assembling the GABARAP interactome. There are many examples of deploying coincident detection to amplify low-affinity protein:lipid interactions (6). Therefore, our findings are compatible with the possibility that GABARAPs and PI4P have synergistic roles in tethering and fusion at physiological PI4P levels, even though this synergy may be less critical when PI4P is greatly increased by shuttling.

PI4P generated by the vertebrate PI4KIIIβ, and its yeast homolog, Pik1, has previously been shown to directly regulate sorting from lysosomes to preserve lysosomal identity (13) and Atg9 Golgi trafficking (17), as well as indirectly by supporting PIP_2 synthesis to promote autophagosome biogenesis (18) and autophagic lysosome reformation (13, 14). Here we show that the PI4P generated by PI4KIIα on autophagosomes has a different and unique role. We hypothesize that this PI4P pool may interact with some of the proteins recently implicated in A:L fusion, such as the novel autophagosomal SNARE syntaxin 17, Rab7 modulators, and interacting proteins (10).

Our findings provide a mechanistic model for integrating two previously unrelated GABARAP functions to promote PI4KIIα- and PI4P-dependent A:L fusion. The unique contributions of PI4KIIα to the GABARAP interactome also raise the intriguing possibility that some of the human disorders ascribed to defects in PI4KIIα (5) may arise partly as a result of dysfunctional PI4KIIα-dependent autophagic clearance.

Materials and Methods

See *SI Materials and Methods* for detailed description.

Reagents and Plasmids. Anti-PI4P and PI4P/PIP_2 Shuttling Kits were from Echelon Bioscience. Plasmids are as described previously. Protein overexpression was kept at a low level by using low plasmid concentrations and short periods of overexpression.

Cell Lines, siRNAs, and Rescue. HeLa cells cultured in DMEM containing 10% (vol/vol) FBS were transfected with epitope-tagged cDNAs using Lipofectamine 2000. Previously validated siRNAs that target human PI4KIIα (6), PIP5Kβ (19), and PI4KIIIβ (20) or Ctrl siRNA were from Sigma. The si*GABARAP/GATE-16* pool was directed against all members of the family (3). In some experiments, a HeLa cell line that stably expresses GFP-LC3 (HeLa/GFP-LC3) or a COS cell line that stably expresses GFP-PI4KIIα was used.

Autophagy Assays. For most experiments, cells were cultured in DMEM/10% (vol/vol) FBS, and autophagy was induced by treatment with EBSS (for 30 min to 2 h) or DMEM/Rap (1 μM, for 2–4 h). In some cases, cells were transferred to Opti-MEM/5% (vol/vol) FBS for 4 h to minimize basal autophagy and were then exposed to autophagic stimuli. Bulk autophagic flux was determined by Western blotting of LC3 or GFP-LC3, and band intensity was quantified using NIH ImageJ software, as described previously (3). LC3 flux was calculated from the intensities of LC3-I and LC3-II bands and normalized against actin loading controls. Autophagosome acidification was determined by transfecting cells with the tandem mRFP-GFP-LC3 fusion construct 24 h after siRNA treatment. Cells were treated with Baf A1 (100 nM) for 12 h, washed to release the Baf A1 block, and fixed at 0, 1, and 3 h with 4% (vol/vol) paraformaldehyde. Puncta with yellow (mRFP+GFP) or red fluorescence were quantified.

Coimmunoprecipitation. HEK-293 cells were cotransfected with myc-PI4KIIα variants, and GFP-Atg8 plasmids were processed for immunoprecipitation using anti-myc or anti-GFP and protein G-agarose and subjected to Western blotting.

Microscopy and Image Analysis. Cells grown on coverslips were processed for immunofluorescence microscopy and examined by laser scanning confocal microscope (Zeiss LSM 510 META UV/Vis). Colocalization analysis and time-lapse recordings were described in *SI Materials and Methods*. HeLa/GFP cells exposed to EBSS were prepared for conventional electron microscopy or correlative light and electron microscopy, as described previously (21).

PI4P/PIP_2 "Shuttling." Cells transfected with siRNA for 48 h were replated on coverslips for 12–24 h. They were washed with serum-free DMEM twice, followed by incubation at 37 °C with ShuttlePIP, as described previously (6). The diC16 PI4P and PIP_2 and their optimized carriers were mixed at a 1:1 molar ratio for 15 min at room temperature before adding to the culture medium to a final phosphoinositide concentration of 50 μM. Autophagy was initiated at the same time as shuttle addition.

ACKNOWLEDGMENTS. We thank Dr. Zevlun Elazar (Weitzmann Institute, Israel) for gifts of the GABARAP, GATE-16, and DSRFP-LAMP1 plasmids and the University of Texas Southwestern Electron Microscopy and Live Cell Imaging Cores for technical support. This work was supported by NIH Grant R01GM66110 and American Heart Association Grant 13GRNT14650022 (to H.Y.) and Cancer Prevention Research Institute of Texas Grant RP120718-P1 and NIH Grants R01CA84254 and R01CA109618 (to B.L.).

1. Shibutani ST, Yoshimori T (2014) A current perspective of autophagosome biogenesis. *Cell Res* 24(1):58–68.
2. Leil TA, Chen Z-W, Chang C-SS, Olsen RW (2004) GABAA receptor-associated protein traffics GABAA receptors to the plasma membrane in neurons. *J Neurosci* 24(50): 11429–11438.
3. Weidberg H, et al. (2010) LC3 and GATE-16/GABARAP subfamilies are both essential yet act differently in autophagosome biogenesis. *EMBO J* 29(11):1792–1802.
4. Behrends C, Sowa ME, Gygi SP, Harper JW (2010) Network organization of the human autophagy system. *Nature* 466(7302):68–76.
5. Balla T (2013) Phosphoinositides: Tiny lipids with giant impact on cell regulation. *Physiol Rev* 93(3):1019–1137.
6. Wang J, et al. (2007) PI4P promotes the recruitment of the GGA adaptor proteins to the trans-Golgi network and regulates their recognition of the ubiquitin sorting signal. *Mol Biol Cell* 18(7):2646–2655.
7. Hammond GRV, Schiavo G, Irvine RF (2009) Immunocytochemical techniques reveal multiple, distinct cellular pools of PtdIns4P and PtdIns(4,5)P(2). *Biochem J* 422(1):23–35.
8. Barylko B, et al. (2009) Palmitoylation controls the catalytic activity and subcellular distribution of phosphatidylinositol 4-kinase IIα. *J Biol Chem* 284(15):9994–10003.
9. Lu D, et al. (2012) Phosphatidylinositol 4-kinase IIα is palmitoylated by Golgi-localized palmitoyltransferases in cholesterol-dependent manner. *J Biol Chem* 287(26):21856–21865.
10. Shen H-M, Mizushima N (2014) At the end of the autophagic road: An emerging understanding of lysosomal functions in autophagy. *Trends Biochem Sci* 39(2):61–71.
11. Kimura S, Noda T, Yoshimori T (2007) Dissection of the autophagosome maturation process by a novel reporter protein, tandem fluorescent-tagged LC3. *Autophagy* 3(5):452–460.
12. Jahreiss L, Menzies FM, Rubinsztein DC (2008) The itinerary of autophagosomes: From peripheral formation to kiss-and-run fusion with lysosomes. *Traffic* 9(4):574–587.
13. Sridhar S, et al. (2013) The lipid kinase PI4KIIIβ preserves lysosomal identity. *EMBO J* 32(3):324–339.
14. Rong Y, et al. (2012) Clathrin and phosphatidylinositol-4,5-bisphosphate regulate autophagic lysosome reformation. *Nat Cell Biol* 14(9):924–934.
15. Salazar G, et al. (2009) Hermansky-Pudlak syndrome protein complexes associate with phosphatidylinositol 4-kinase type II α in neuronal and non-neuronal cells. *J Biol Chem* 284(3):1790–1802.
16. Jović M, et al. (2012) Two phosphatidylinositol 4-kinases control lysosomal delivery of the Gaucher disease enzyme, β-glucocerebrosidase. *Mol Biol Cell* 23(8):1533–1545.
17. Wang K, et al. (2012) Phosphatidylinositol 4-kinases are required for autophagic membrane trafficking. *J Biol Chem* 287(45):37964–37972.
18. Moreau K, Ravikumar B, Puri C, Rubinsztein DC (2012) Arf6 promotes autophagosome formation via effects on phosphatidylinositol 4,5-bisphosphate and phospholipase D. *J Cell Biol* 196(4):483–496.
19. Chen MZ, et al. (2009) Oxidative stress decreases phosphatidylinositol 4,5-bisphosphate levels by deactivating phosphatidylinositol- 4-phosphate 5-kinase β in a Syk-dependent manner. *J Biol Chem* 284(35):23743–23753.
20. Chu KME, Minogue S, Hsuan JJ, Waugh MG (2010) Differential effects of the phosphatidylinositol 4-kinases, PI4KIIα and PI4KIIIβ, on Akt activation and apoptosis. *Cell Death Dis* 1:e106.
21. Orvedahl A, et al. (2011) Image-based genome-wide siRNA screen identifies selective autophagy factors. *Nature* 480(7375):113–117.